High Pressure Crystallization of HDPE Droplets

Robert Masirek,[†] Ewa Piorkowska,*[,†] Andrzej Galeski,[†] Anne Hiltner,[‡] and Eric Baer[‡]

Centre of Molecular and Macromolecular Studies, Polish Academy of Sciences, 90 363 Lodz, Poland, and Department of Macromolecular Science and Center for Applied Polymer Research, Case Western Reserve University, Cleveland, Ohio, 44106-7202

Received April 25, 2008; Revised Manuscript Received August 11, 2008

ABSTRACT: Dispersions of high density polyethylene (HDPE) particles in polystyrene (PS) were produced by interfacially driven breakup of nanolayers in multilayered systems that were fabricated by means of layer-multiplying coextrusion. The droplet size distribution was controlled by the HDPE initial individual layer thickness: 14, 40 or 120 nm. These unique systems allowed us to demonstrate unequivocally for the first time that the HDPE pseudohexagonal phase formation required nucleation on foreign surfaces or on crystals formed in the orthorhombic form at atmospheric pressure. The dispersions of HDPE particles in the PS matrix were subjected to annealing at high pressure of 480 MPa at 235 °C, in conditions where the pseudohexagonal phase forms in HDPE. To reach the desired conditions the samples were first heated and then subjected to high pressure or they were first pressurized and then heated. The samples treated according to the first route melted and transformed into the pseudohexagonal phase from the molten state whereas the second route allowed for transformation of orthorhombic crystals to the pseudohexagonal phase without previous melting. The lamella thickness formed under high pressure was estimated on the basis of melting temperature. The HDPE particles, annealed under high pressure without previous melting, exhibited high melting temperature, above 140 °C, corresponding to the lamella thickness above 50 nm, that indicated thickening in the pseudohexagonal phase. The HDPE particles that were first melted and then pressurized behaved differently depending on their sizes: thick lamellae were formed under high pressure only in particles large enough to contain heterogeneities able to nucleate HDPE bulk crystallization. These results point out that nucleation, presumably heterogeneous, is advantageous, or even necessary, for the formation of the HDPE pseudohexagonal phase.

Introduction

Under high pressure, above 300 MPa, polyethylene (PE) forms a two-dimensional pseudohexagonal phase, which also has been claimed to be a precursor phase in crystallization of the usual orthorhombic form even at atmospheric pressure.[1] The conditions of the pseudohexagonal phase stability are defined by the phase diagram; the required temperature for pseudohexagonal phase stability is also high, usually above 220 °C. Upon cooling under elevated pressure the pseudohexagonal phase transforms to the crystalline orthorhombic form. A metastable pseudohexagonal phase can also form within the orthorhombic-stable region, for instance it is formed when PE crystallizes at high pressure during cooling at a rate 1 °C/min.[1] Based on Raman spectra of the pseudohexagonal phase the presence of a large amount of kink conformational defects of the kind TG±TG± within an otherwise fully trans-planar chain was inferred.[2]

Weak interactions between chains within the pseudohexagonal phase enable sliding diffusion that leads to gradual thickening of the ordered domains reaching thicknesses significantly larger than that of lamellae crystallized directly into the orthorhombic form. Melt crystallized orthorhombic crystals transferred into the region of pseudohexagonal phase stability, first by increasing pressure and then temperature, transform into pseudohexagonal domains and thicken considerably.[1,3] The thickness of crystals that crystallized or thickened in the pseudohexagonal phase is larger than that of melt crystallized orthorhombic crystals and usually exceeds 50 nm.[1] However, Bassett and Khalifa[4] demonstrated that film thickness affected the thickness of crystals formed in the pseudohexagonal phase. In 3 μm thick films it was 142 nm, significantly smaller than that in the bulk polymer, subjected to the same treatment, which was 307 nm. Moreover, Khalifa and Bassett[5] reported high pressure annealing of solution grown orthorhombic crystals that resulted in 30 nm thick pseudohexagonal crystals. Such small thickness resulted from severe confinement in 30 nm thick domains.

The mesomorphic phase of isotactic polypropylene forms at high supercooling, below 60 °C via homogeneous mechanism.[6,7] The pseudohexagonal phase of PE, having also mesomorphic character, forms at low supercooling that might suggest that heterogeneous rather than homogeneous nucleation is active. The present paper is aimed at answering this question by studying high pressure crystallization in PE droplets.

Polymer droplets are long known to solidify via fractionated crystallization[8−14] reflected in the presence of more than one crystallization exothermic peak. The lowest temperature exothermic peak with the largest supercooling is usually associated with homogeneous nucleation while exothermic peaks at higher temperatures are attributed to crystallization from nuclei formed on active heterogeneities. Recently Bernal-Lara et al.[15] studied multilayered systems of high density polyethylene (HDPE) and atactic polystyrene (PS) fabricated by means of layer-multiplying coextrusion that uses forced assembly to create thousands of alternating layers of two polymers.[16] Heating films above the melting temperature of HDPE resulted in breakup of HDPE layers into droplets followed by fractionated crystallization during subsequent cooling. The droplet size, hence the crystallization behavior, was controlled by the individual HDPE layer thickness. The droplets formed by melting of the thinnest 14 nm layers were numerous enough that the majority did not contain an active heterogeneity and crystallization occurred at about 80 °C, which was interpreted as a result of homogeneous nucleation. We note that the lowest crystallization temperature reported for HDPE is around 70 °C.[13] The differences in reported temperatures of fractionated crystallization of HDPE

* Author to whom correspondence should be addressed. E-mail: epiorkow@bilbo.cbmm.lodz.pl.
† Polish Academy of Sciences.
‡ Case Western Reserve University.

10.1021/ma800933g CCC: $40.75 © 2008 American Chemical Society
Published on Web 10/07/2008

originate from the complexity of this phenomenon; a polymer may contain several types of heterogeneities with different levels of activity, and a surface nucleation is also possible. However, the interface might also hinder the crystallization in adjacent nanolayers.[17] The aim of this work was to study the formation of the pseudohexagonal phase in HDPE droplets depending on the droplet size. We prepared dispersions of HDPE with different droplet sizes by heating HDPE/PS nanolayered films with various initial thickness of individual HDPE layers. The HDPE droplets embedded in PS were subjected to appropriate high pressure and temperature treatment to reach the region of pseudohexagonal phase formation and stability in the phase diagram. Subsequent DSC studies allowed differentiation between thick crystals thickened while residing in the pseudohexagonal phase and thin crystals crystallized directly from melt into the usual orthorhombic form.

Experimental Section

Materials and Samples. The studies employed multilayered films with 257 alternating layers of a high density polyethylene (HDPE) and polystyrene (PS) extruded on a laboratory scale coextrusion line at Case Western Reserve University that incorporates layer-multiplying technology.[15,16] The metallocene high density polyethylene with bulk density of 0.9538 g cm^{-3}, M_w of 125 000, and melt flow index of 0.8 g/10 min according to ASTM D1238 was provided by the Dow Chemical Company. The polystyrene was Dow STYRON 685D (M_w of 527 000) with bulk density of 1.0450 g cm^{-3} according to ASTM D792 and melt flow index of 1.5 g/10 min. The studies focused on three systems: two of them with the HDPE-to-PS volumetric feed ratio 10:90, 152 μm thick HDPE/PS-1 and 51 μm thick HDPE/PS-2, and one with the HDPE-to-PS volumetric ratio 5:95, 18 μm thick HDPE/PS-3. The detailed characterization including AFM images of these films was given in ref 15. HDPE layers in HDPE/PS-1 and HDPE/PS-2 were continuous, and their thickness measured by atomic force microscopy was close to the nominal layer thickness of 120 and 40 nm, respectively. In HDPE/PS-3 considerable layer breakup occurred, and the thickness of the HDPE layer fragments was 14 nm, higher than the nominal thickness, due to retraction of the fractured layers. The HDPE film and PS control film, both 305 μm thick, were also coextruded and studied for comparison.

Methods. In the studies a scanning differential calorimeter, TA Instruments DSC 2920, was used. Specimens of HDPE, PS, HDPE/PS-2 and HDPE/PS-3 films having mass of about 20 mg were heated at 10 °C/min to 200 °C, annealed for 1 min and cooled at 10 °C/min to room temperature under a nitrogen flow. This protocol made it possible to break up the HDPE layers and to crystallize the droplets. Preliminary studies demonstrated that accomplishment of HDPE layer breakup in HDPE/PS-1 required a longer annealing time at 200 °C, about 10 min. In order to check reproducibility of the crystallization process the heating and cooling cycles were repeated. Several such 20 mg specimens containing droplets of HDPE embedded in PS matrix were assembled into packages weighing 60−70 mg and used as samples for further high pressure crystallization. These samples after annealing at high pressure were also subjected to heating and cooling cycles, that allowed us to study their melting and crystallization behavior.

A crystallinity level and lamellar thickness l were estimated on the basis of the heat of melting and melting peak temperature T_m, respectively. For the determination of lamellar thickness, the Gibbs−Thompson equation was used:[18]

$$l = 2\sigma_e T_m^\circ / \Delta h_f (T_m^\circ - T_m) \quad (1)$$

where σ_e is the lamellar basal-surface free energy (for PE $\sigma_e = 90$ mJ/m^2),[19] T_m° is the extrapolated equilibrium T_m equal to145.1 °C, as measured earlier by us for Petrothene LS 606-00 PE[20] whereas Δh_f is the heat of fusion per unit volume (for PE, $\Delta h_f = 293$ J/cm^3).[21] The same value of Δh_f was used to calculate a crystallinity level from the melting enthalpy.

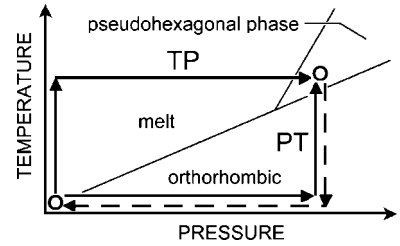

Figure 1. The two routes, TP and PT, used to reach the pseudohexagonal phase stability region on the PE phase diagram.

The high pressure cell described in detail in refs 3 and 22 was made of ultra-high-strength steel capable of applying pressure up to 1 GPa at the temperature up to 320 °C. Four electrical heaters (600 W total power) were controlled by a temperature controller, which ensured a temperature accuracy of 1 °C inside the cell. The temperature sensor was placed 10 mm away from the sample in a narrow 1 mm thick channel, perpendicular to the wall of the cell. The polymer was compressed by the use of an Instron tensile testing machine (Instron Corp., High Wycomb, U.K.), via a fixture that stabilized the load exactly along the cell axis. The hydrostatic pressure inside the cell was controlled by means of a tensile testing machine with an accuracy of ±0.5 MPa. The velocity of the cross head of the tensile testing machine was 2 mm/min.

The high-pressure transformation of the samples containing HDPE droplets in a PS matrix was performed by annealing at the elevated temperature of 235 °C, under the high pressure of 480 MPa. These conditions were selected based on the preliminary studies and the previous works.[3,22] Additional experiments were conducted during which the samples were annealed at 225 or at 230 °C. Two routes, illustrated in Figure 1, were used to reach the desired conditions: (1) The samples were first heated and then subjected to high pressure, the TP route; and (2) the samples were first pressurized and then heated to a desired temperature, the PT route.

The samples treated according to the TP route melted and solidified in the pseudohexagonal phase from the molten state. The PT route allowed for transformation of the orthorhombic crystals into the pseudohexagonal phase and for thickening of domains without previous melting. After annealing under high pressure for 1 or 2 h, the samples were cooled down to room temperature, and then the pressure was released.

Structure of the samples was examined by scanning electron microscopy (SEM), using a Jeol 5500 L operating in high vacuum and with accelerating voltage of 10 kV. To expose the interior of HDPE/PS systems the samples were broken in the liquid nitrogen temperature. Prior to SEM examination the samples were sputtered with gold.

The SEM technique was also utilized to measure the size distribution of HDPE droplets in HDPE/PS system after the HDPE layers breakup in the DSC. Since fracture may propagate preferentially through the interface of PS and larger HDPE particles, we devised a procedure for removal of the PS matrix. 300 mg of each material was dissolved in toluene to 0.6 wt % concentration. The solution was then centrifuged at 23 °C for 2 h at an acceleration of 2859 g in a centrifuge T21 Sorvall. The supernatant liquid was removed, fresh toluene was added to the sediment and the suspension was subjected to ultrasonic excitation. To remove PS completely from the suspension of HDPE droplets, the centrifugation and redispersion was repeated 3 times. After the third centrifugation only a small amount of toluene was added to the sediment and a drop of suspension was deposited on the surface of the SEM specimen holder. The solvent was removed and each specimen was examined under the SEM after gold sputtering. In each case, the diameters of about 500 HDPE particles were

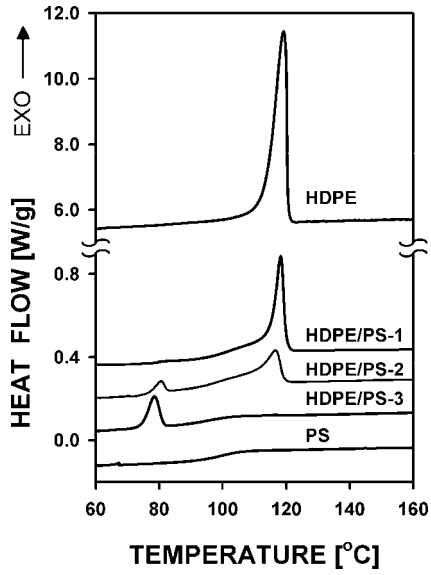

Figure 2. DSC cooling thermograms recorded for HDPE/PS, HDPE and PS control films.

Table 1. Crystallization Behavior of HDPE/PS Systems[a]

sample code	T_{c1} [°C]	T_{c2} [°C]	ΔH_{c1} [J/g of HDPE]	ΔH_{c2} [J/g of HDPE]
HDPE	119		194	
HDPE/PS-1	118	81.5	128	1.4
HDPE/PS-2	116	80.5	98	18
HDPE/PS-3	116	78	12	86

[a] T_{c1} and T_{c2}, ΔH_{c1} and ΔH_{c2} denote crystallization temperatures and enthalpies associated with high and low temperature exotherms, respectively.

measured on SEM micrographs in order to determine a particle size distribution.

In addition, the morphology of HDPE control samples annealed under high pressure was investigated by SEM. To expose the internal structure the samples were cut and the surfaces were treated with a permanganate etchant according to the procedure developed originally by Olley and Bassett.[23] We prepared reagents by dissolving 1 wt % potassium permanganate in a mixture of one part by volume of concentrated sulfuric acid and one part of concentrated orthophosphoric acid. The etching was conducted at room temperature for 30 min. Then, the samples were carefully washed applying the procedure described elsewhere.[23]

Results and discussion

Heating the HDPE/PS nanolayered films in the DSC above the melting temperature of HDPE resulted in breakup of the HDPE layers into droplets. Subsequent crystallization of the HDPE droplets produced the cooling thermograms in Figure 2.

The control HDPE and PS films are included for comparison, and the relevant calorimetric data are collected in Table 1. The crystallization enthalpy values are averaged over 3−5 samples. The HDPE control showed a crystallization peak at around 119 °C. HDPE/PS systems exhibited fractionated crystallization with two crystallization exothermic peaks, the usual one at T_{c1} of 116−118 °C and another with very high supercooling at T_{c2} at about 78−82 °C.

These exotherms corresponded to crystallization of the droplets from different nuclei, as it was described in ref 15. Moreover, for HDPE/PS-1 the low temperature exothermic peak, and for HDPE/PS-3 the high temperature one were very low and poorly reproducible. HDPE in HDPE/PS-1 crystallized predominantly from nuclei formed on very active heterogeneities whereas in HDPE/PS-3 from nuclei requiring much lower temperature, as can be judged from the relations between the

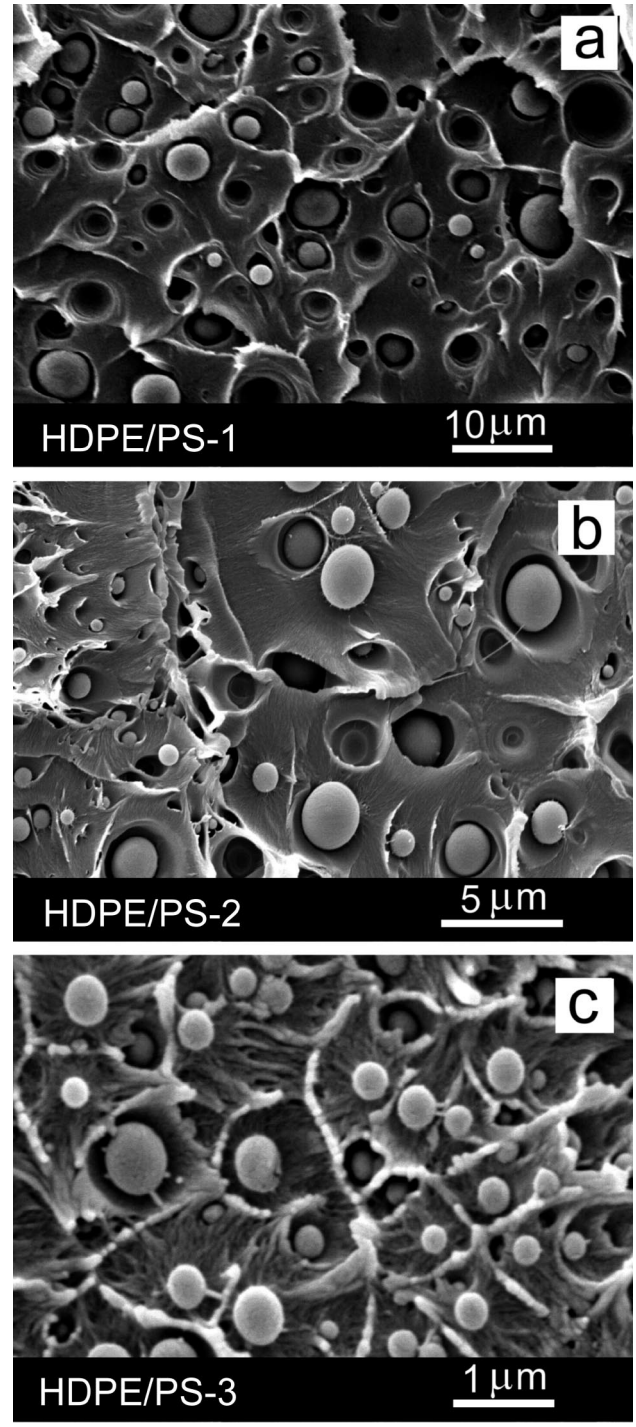

Figure 3. SEM micrographs of cryo-fracture surfaces of HDPE/PS systems after the first cooling in DSC: (a) HDPE/PS-1; (b) HDPE/PS-2; (c) HDPE/PS-3.

enthalpies associated with the corresponding crystallization exothermic peaks. The droplets in HDPE/PS-2 crystallized from both types of nuclei although the crystallization nucleated by very active heterogeneities prevailed. We note that repeating the heating/cooling cycle practically had no influence on the crystallization behavior of the systems; the crystallization exotherms during the first and the second cooling did not differ.

Figure 3 shows SEM micrographs of cryo-fracture surfaces of HDPE/PS system after the first cooling scan in the DSC. As expected, the HDPE layers broke into droplets of sizes dependent on individual HDPE layer thickness. The largest droplets as determined from such micrographs were 11, 2.8 and 1 μm

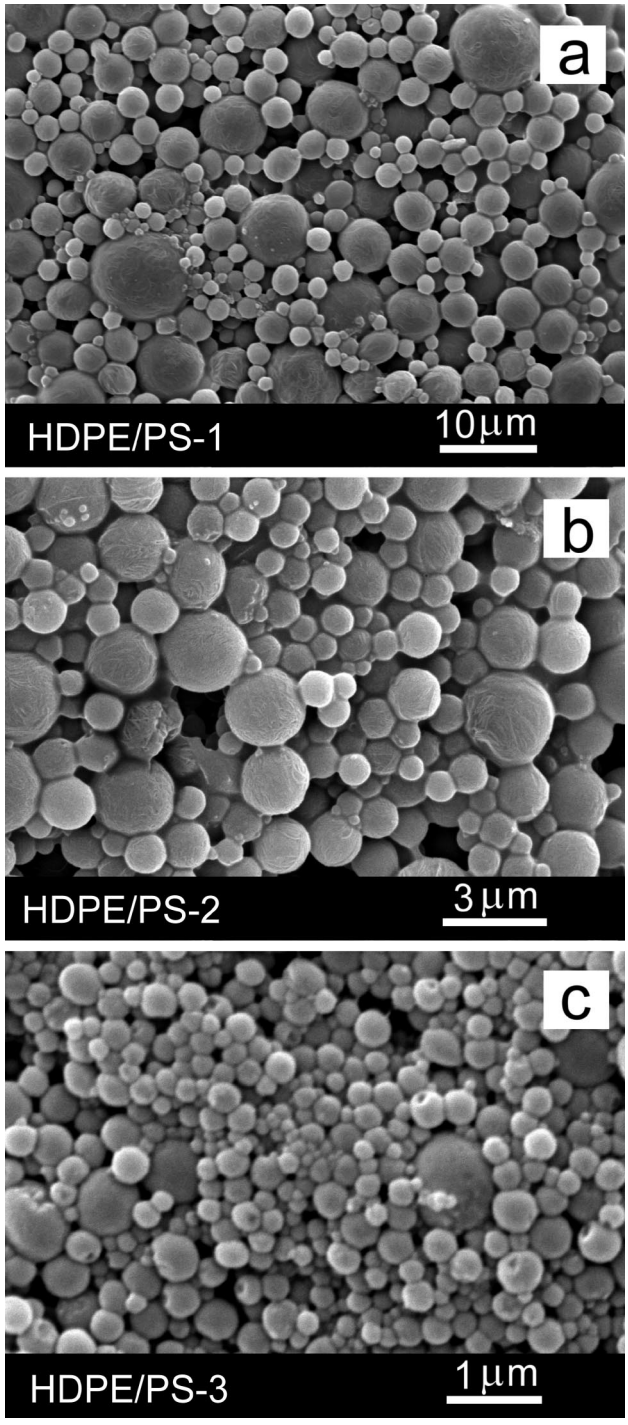

Figure 4. SEM micrographs of isolated HDPE particles from (a) HDPE/PS-1; (b) HDPE/PS-2; (c) HDPE/PS-3.

in size for HDPE/PS-1, HDPE/PS-2 and HDPE/PS-3, respectively.

Figure 4 shows SEM micrographs of HDPE particles extracted from the PS matrix, whereas size distributions of the particles are displayed in Figure 5.

The volume average size was 6.4, 1.86 and 0.53 μm for particles in HDPE/PS-1, HDPE/PS-2 and HDPE/PS-3, respectively. The particles in HDPE/PS-3, of diameter less than 1 μm, were sufficiently numerous and small that most of them were free from active heterogeneities that nucleated HDPE crystallization in bulk. Particles of this size constituted only 15% of the total HDPE volume in HDPE/PS-2 and less than 1% of the total HDPE volume in HDPE/PS-1.

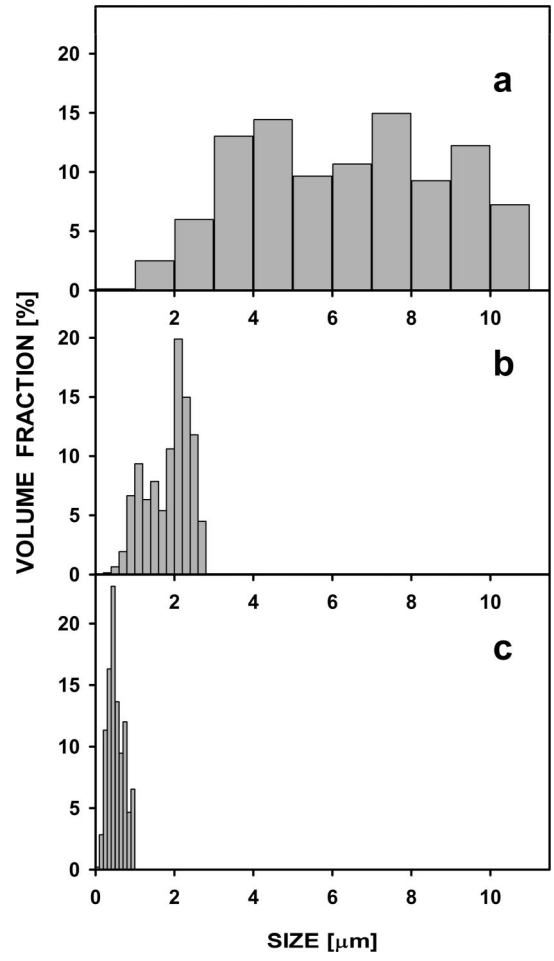

Figure 5. Size distributions of HDPE particles in (a) HDPE/PS-1; (b) HDPE/PS-2; (c) HDPE/PS-3.

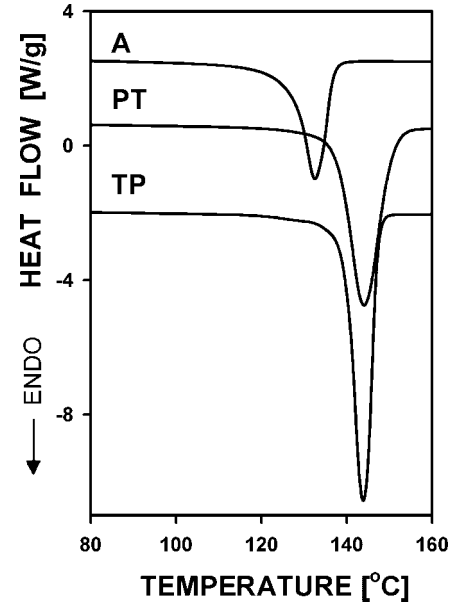

Figure 6. Heating thermograms of HDPE samples: control film, unannealed (A) and annealed under high pressure 480 MPa at 235 °C for 1 h: treated according to PT and TP routes as indicated in the figure.

Figure 6 shows exemplary DSC traces of the HDPE control films unannealed and annealed under high pressure whereas the relevant calorimetric data are collected in Table 2. The thermogram for the unannealed sample exhibited typical HDPE

Table 2. Melting Behavior of HDPE and HDPE/PS Systems, Unannealed (A) and Annealed for 1 or 2 h under High Pressure, Reached by TP or PT Route, as Indicated[a]

sample code	T_{m1} [°C]	T_{m2} [°C]	l_1 [nm]	l_2 [nm]	ΔH_{m1} [J/g of HDPE]	ΔH_{m2} [J/g of HDPE]	c [%]
HDPE							
A	133.2		21.6		181		62
TP, 1 h		144.5		428		284	97
TP, 2 h		144.6		514		287	98
PT, 1 h		144.05		245		283	97
PT, 2 h		144.1		257		284	97
HDPE/PS-1							
A	134.1		23.4		128		44
TP, 1 h	131.5, 134.5	142.8	18.9,24.2	112	71	94	56
TP, 2 h	131.5, 134.6	142.8	18.9,24.5	112	72	95	57
PT, 1 h		141.6		73.4		212	72
PT, 2 h		141.6		73.4		216	74
HDPE/PS-2							
A	131.3		18.6		114		39
TP, 1 h	131.2	142.6	18.5	103	103	40	49
TP, 2 h	130.9	142.5	18.1	98.8	104	39	49
PT, 1 h	130.0	141.0	17.0	62.7	6	207	73
PT, 2 h		141.4		69.4		208	71
HDPE/PS-3							
A	130.8		17.9		102		35
TP, 1 h	130.5	142.2	17.6	88.6	104	8	38
TP, 2 h	130.5	142.2	17.6	88.6	105	7	38
TP, 2 h*	130.4	142.4	17.5	95.2	101	7	37
PT, 1 h	129.5	140.0	16.5	50.4	8	174	62
PT, 2 h	129.5	140.1	16.5	51.4	9	183	65

[a] T_{m1} and T_{m2}, ΔH_{m1} and ΔH_{m2} denote melting temperatures and enthalpies associated with high and low temperature endotherms, respectively. The asterisk denotes the sample annealed at 230 °C.

melting behavior, that is, a melting peak centered at $T_m = 133.2$ °C, corresponding to lamella thickness of 22 nm, and crystallinity level of 62%. The HDPE samples annealed under high pressure exhibited high T_m and large crystallinity levels, exceeding those of the unannealed sample. High T_m indicated the large lamella thickness, hence the crystals thickened in the pseudohexagonal phase.

The TP route led to the formation of the pseudohexagonal phase directly from the melt. The PT route caused transformation of the orthorhombic crystals into the pseudohexagonal phase and thickening in this phase. In both cases the lamella thickness of the pseudohexagonal form was conserved when the pseudohexagonal phase transformed to the orthorhombic phase upon cooling under pressure. The PT route resulted in lower T_m and thinner lamellae than in the case of the TP route. In the latter case, the melting peak was also sharper indicating more uniform lamella thickness. Differences in the melting behavior between HDPE samples reflected their different history and different mechanism of crystal formation. Regardless of the applied route an increase of annealing time from 1 to 2 h had little effect on T_m or on the crystallinity level.

SEM examination of permanganate etched samples confirmed the presence of very thick lamella in HDPE annealed under high pressure as shown in Figure 7.

Figure 8 shows the heating thermograms of HDPE/PS samples containing droplets of HDPE whereas the heating thermograms of these samples annealed under high pressure are collected in Figures 9 and 10 for both TP and PT routes, respectively. The relevant calorimetric data are listed in Table 2.

All HDPE/PS systems annealed under high pressure, which was reached via the TP route, exhibited complicated melting behavior. In each case the relevant thermogram featured two melting endotherms as shown in Figure 9 although for HDPE/PS-3 the high temperature melting peak was very small and hardly recognizable. The high temperature melting endotherms with peaks at 142.2−142.8 °C resulted from melting of thick crystals, of thickness in the range 88−112 nm which, obviously

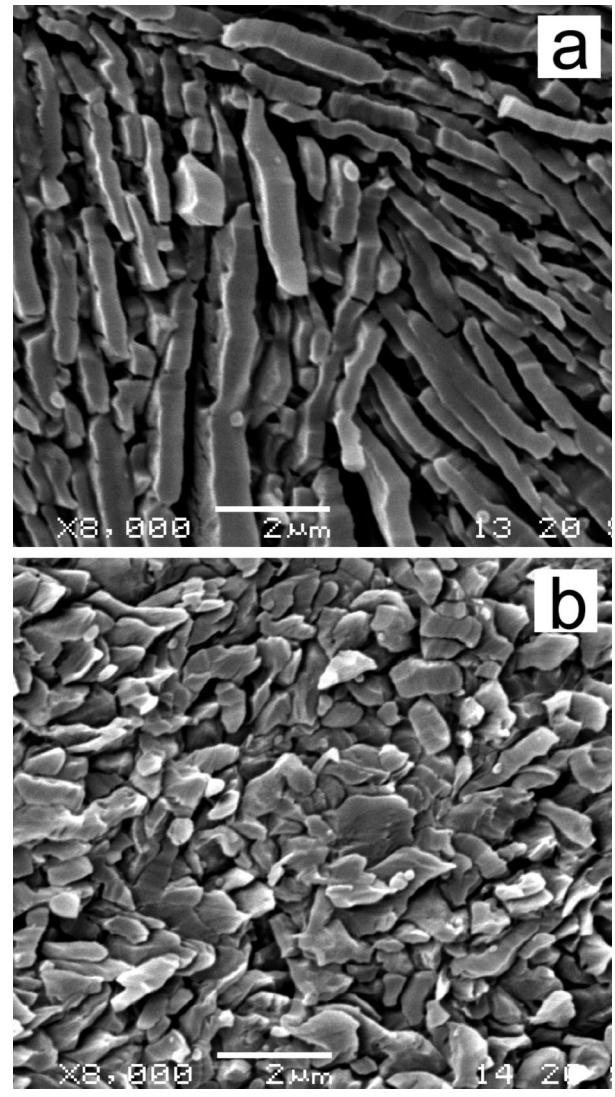

Figure 7. SEM microphotographs of etched HDPE samples annealed under high pressure of 480 MPa at 235 °C for 1 h according to (a) TP route, (b) PT route.

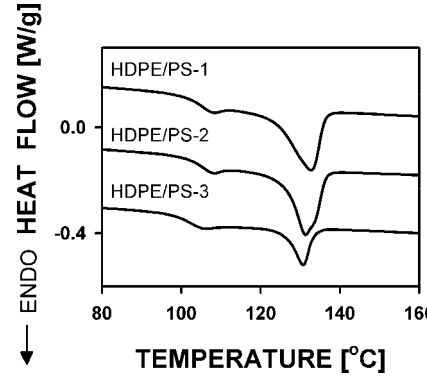

Figure 8. Heating thermograms of HDPE/PS systems containing HDPE droplets.

crystallized in the pseudohexagonal phase under high pressure. The low temperature melting endotherm featured two peaks in the case of HDPE/PS-1, and single peaks in the case of HDPE/PS-2 and HDPE/PS-3. T_m values determined from these peaks are in the range of 130.4 to 134.6 °C, and correspond to rather typical thickness of PE lamellae, ranging from 17 to 24.5 nm. The small crystal thickness suggests that this fraction of crystals was formed during cooling in the usual orthorhombic form. We

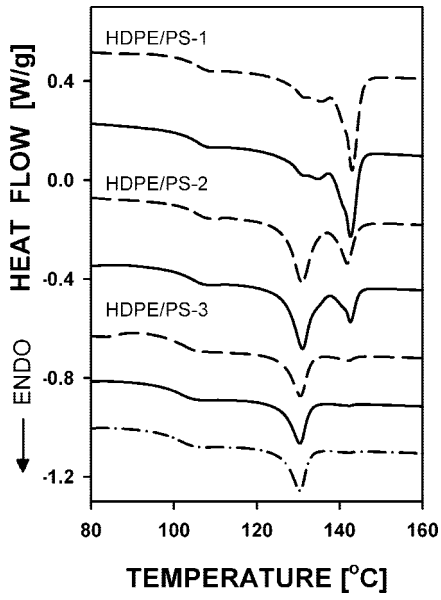

Figure 9. Heating thermograms of HDPE/PS systems with HDPE particles dispersed in PS matrix annealed under high pressure 480 MPa at 235 °C for 1 h (dashed line) or 2 h (solid line). Dash-dotted line: thermogram of HDPE/PS-3 annealed at 230 °C. All samples were treated according to the TP route.

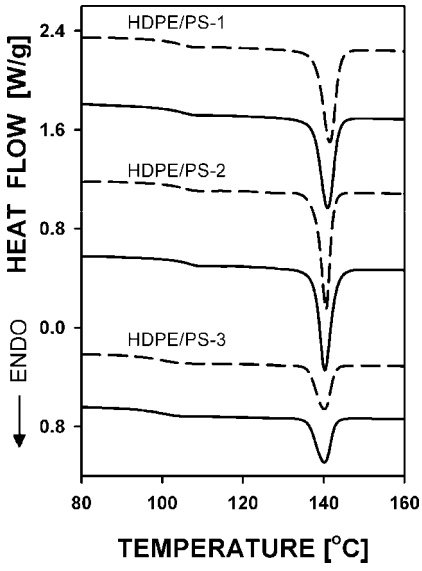

Figure 10. Heating thermograms of HDPE/PS systems with HDPE particles dispersed in PS matrix annealed under high pressure 480 MPa at 235 °C for 1 h (dashed line) or 2 h (solid line). All samples were treated according to the PT route.

note that the size of the HDPE droplets exceeded by at least 1 order of magnitude the thickness of domains in which 30 nm thick pseudohexagonal crystals were reported.[4]

The melting enthalpy values associated with low and high temperature melting endotherms listed in Table 2 show that the fraction of thick crystals prevailed in HDPE/PS-1. It was still significant in HDPE/PS-2, contributing to approximately 1/3 of the melting enthalpy, but in HDPE/PS-3 it decreased only to 6−7% of the total mass of crystals. The total melting enthalpy, hence the crystallinity level, decreased in parallel with the decreasing fraction of thick crystals being the largest for HDPE/PS-1 and the smallest for HDPE/PS-3.

Figure 10 shows a collection of heating thermograms of HDPE/PS samples annealed under high pressure that was reached via the PT route. The thermograms are featured by high

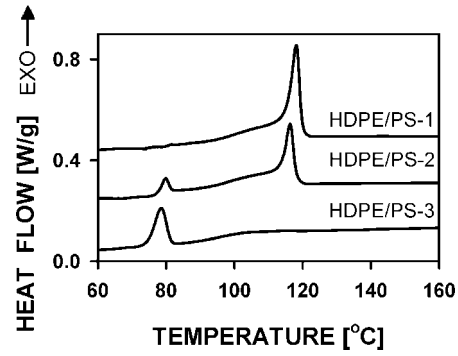

Figure 11. Cooling thermograms of HDPE/PS systems that were annealed under high pressure of 480 MPa at 235 °C for 2 h according to TP route, and next heated and cooled in the DSC.

temperature melting peaks centered at 140.0−141.6 °C that indicate the lamella thickness in the range of 50−74 nm. The melting enthalpy, above 180 J/g of HDPE, indicates a relatively high crystallinity level, above 60%, in HDPE droplets. The thermograms of HDPE/PS-3 and the thermogram of HDPE/PS-2 annealed under high pressure for 1 h exhibited also very small low temperature melting endotherms with T_{m1} at 129.5−130 corresponding to melting of a small amount of thin crystals. The crystallinity level and the lamella thickness of thick crystals in HDPE droplets were smaller than these in the HDPE control sample, which reflects the influence of spatial confinement on the thickening of pseudohexagonal domains. The thick crystal thickness was also smaller than that of thick crystals in corresponding samples that were subjected to high pressure via the TP route. However, the same applies also to the HDPE control sample. Obviously the thickening of crystals is easier during the growth from the melt than when they are constrained by other crystals.

We note that neither increasing the high pressure annealing time to 2 h nor decreasing the annealing temperature to 230 °C resulted in any significant changes of the melting behavior of the HDPE/PS systems.

After heating in the DSC to 200 °C, all the samples were cooled again to room temperature at 10 °C/min. The cooling thermograms shown in Figure 11 showed that the melting erased the thermal history and the crystallization of HDPE droplets proceeded as before the high pressure crystallization (compare Figure 2). The fractionated crystallization indicated that the fractions of HDPE droplets crystallizing from different nuclei did not change in the studied systems annealed under high pressure.

Figure 12 shows exemplary SEM micrographs of cryo-fracture surfaces of HDPE/PS samples after 2 h of annealing under high pressure. HDPE droplets visible in these micrographs are of the same size as those in Figure 3. Reproducibility of crystallization behavior and SEM studies indicated stability of the HDPE dispersions in the PS matrix during high pressure experiments and subsequent DSC heating and cooling scans. The shown examples concern the samples treated according to TP route, but the same results were obtained for the samples which were subjected to high pressure and temperature by the PT route.

The results showed that the pseudohexagonal phase formed from the melt (TP route) only in those HDPE/PS systems that under atmospheric pressure crystallized from heterogeneous nuclei, similarly as the bulk polymer. The pseudohexagonal phase practically did not form in HDPE/PS-3 that is in the submicron HDPE droplets that were sufficiently small and numerous that most of them were free from active heterogeneities that nucleated HDPE bulk crystallization under atmospheric pressure. The pseudohexagonal phase was formed from

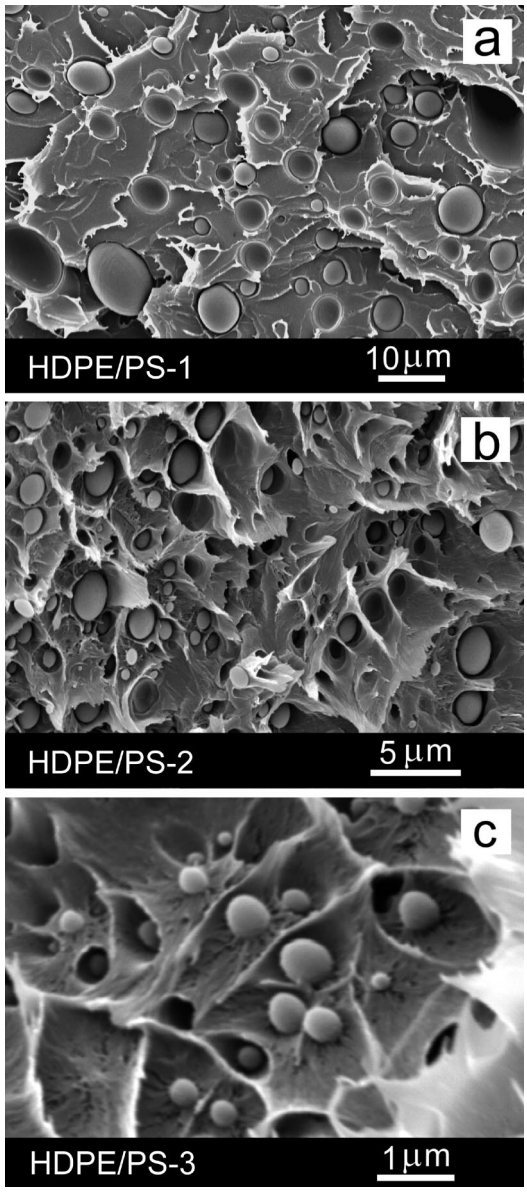

Figure 12. SEM micrographs of cryo-fracture surfaces of HDPE/PS systems after annealing under high pressure of 480 MPa at 235 °C for 2 h according to the TP route: (a) HDPE/PS-1; (b) HDPE/PS-2; (c) HDPE/PS-3.

the molten state only in the larger HDPE particles that were present in HDPE/PS-1 and HDPE/PS-2 systems, where the crystallization, similar to that in the bulk polymer, prevailed under atmospheric pressure. This indicated that the nucleation on active heterogeneities was necessary for the formation of the pseudohexagonal phase under high pressure crystallization from the melt.

However, the mass fraction of pseudohexagonal domains formed under high pressure that was reached via the TP route is around 60% and 30% of the total crystallinity for HDPE/PS-1 and HDPE/PS-2, respectively. These numbers are smaller than those for crystals heterogeneously nucleated at 116−118 °C under atmospheric pressure being 99% and 84% of the total crystallinity for these systems, respectively. There are two possible reasons for this discrepancy. Possibly, not all the impurities that are able to nucleate efficiently the orthorhombic form nucleate also the pseudohexagonal phase. Moreover, the orthorhombic phase crystallizes in the form of spherulites growing from the nuclei and occupying the entire available space. The pseudohexagonal phase does not form radially growing spherulites and is arranged into domains containing thick parallel lamellae as it is seen in Figure 7a. Lamella branching is rare, and there is no radial growth. The pseudohexagonal domains do not fill the entire volume of HDPE droplets as spherulites do, leaving thus room for the orthorhombic phase which crystallizes upon cooling.

The changes in the various fractions of the HDPE as a function of temperature under pressure were measured in the past by Prins et al. and described in a series of papers.[24−26] They employed solid state NMR spectroscopy under high pressure to identify the three coexisting phases of HDPE: amorphous, orthorhombic and pseudohexagonal by measuring proton-NMR spin−lattice relaxation rates. During the first run under high pressure, the temperature was increased step-by-step while monitoring the sample composition using various deuteron NMR experiments. In this way the transition from the orthorhombic phase to the hexagonal phase and the melting transition were observed. The surprising fact discovered by de Langen et al.[25] was that the pseudohexagonal phase coexisted with the orthorhombic phase almost up to the melting point, and that the amount of pseudohexagonal material was not very large, up to 60% of the total mass. In the second run the temperature was decreased from 250 °C (in the liquid phase) to 200 °C (in the orthorhombic phase). The pseudohexagonal phase showed up in the NMR spectrum at 232 °C. The orthorhombic component appeared at 230 °C and grew at the expense of the pseudohexagonal component until, at 215 °C, all pseudohexagonal material disappeared. The maximum amount of pseudohexagonal phase exceeded slightly 40%. However, the complete equilibrium could not be achieved in practice,[25] as suspected by the authors, due to very long crystallization times. An indication that real equilibrium was not achieved was the observation that the phase transitions occurred at different temperatures depending on whether the temperature was increased or decreased. Now we learned that the real reason for the observed difference is that nucleation, presumably heterogeneous, was needed for the formation of the pseudohexagonal phase from the melt.

Annealing under high pressure reached via the PT route in each case resulted in marked crystal thickening. Thus, the spatial constraints did not prevent the thickening of existing crystals in the pseudohexagonal phase. However, the crystal thickness, in the range of 50−74 nm, and the crystallinity level in HDPE droplets, 62−74%, were below those in the HDPE control sample. Moreover, the crystal thickness decreased with decreasing HDPE droplet size. In the samples treated according to the TP route the crystals in the thick crystal fraction were thicker but they also did not attain the thickness of crystals in the HDPE control sample and the thickness exhibited a tendency to decrease with a decrease of HDPE particle size. Therefore, although the spatial constraints did not prevent crystal thickening, nevertheless they limited the thickness of pseudohexagonal domains. This is a surprising result because the droplet size exceeds the thickness of crystals formed under high pressure in the HDPE control samples. Even in HDPE/PS-3 the droplets larger than 0.5 μm constitute approximately 50 vol %.

We emphasize here that at 230 or 235 °C, under the pressure of 480 MPa, PS is above its glass transition temperature, T_g. Oels and Rehage[27] studied the glass transition of PS under pressure up to 400 MPa. Extrapolation of their results gives an estimated T_g of PS under the pressure of 480 MPa of about 208 °C. Although the glass transition of PS broadens under high pressure, it is still below 230 °C. Thus HDPE droplets under the pressure of 480 MPa were surrounded by PS in the rubbery state that enabled efficient pressure transfer. It is therefore clear that in samples that were first heated to 235 °C or to 230 °C

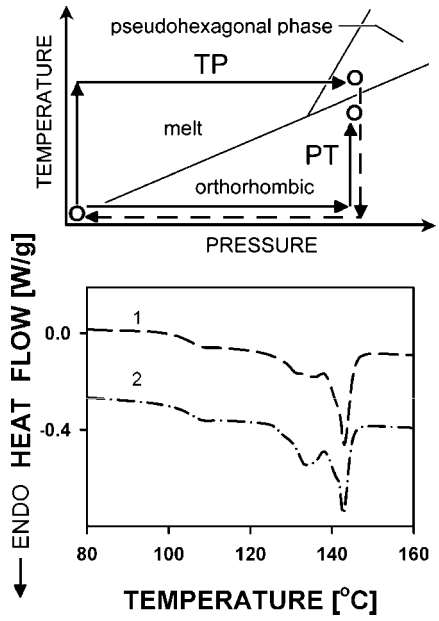

Figure 13. Heating thermograms of HDPE/PS-3 system with HDPE particles dispersed in PS matrix: (1) annealed under 480 MPa at 235 °C for 1 h according to TP route, (2) annealed under 480 MPa at 235 °C for 1 h according to TP route, cooled to room temperature and then annealed under 480 MPa at 225 °C for 1 h according to PT route as drawn in the scheme above.

and then pressurized, up to 480 MPa, the HDPE droplets were subjected to hydrostatic pressure.

While applying the PT route we intended to induce a transformation of orthorhombic crystals directly to the pseudohexagonal phase avoiding melting. We admit that the transfer of the pressure to HDPE inclusions could be worse in samples treated according to the PT route, when the pressure is applied to a system with glassy PS. Nevertheless the increase in pressure, even if not to a desired value, resulted in elevation of the melting temperature of HDPE crystals. When the temperature reached the region of the PS glass transition and PS softened, the transfer of pressure to the HDPE particles was improved and upon further heating the conditions of the pseudohexagonal phase stability were reached. To prove further this scenario we carried out an experiment with the HDPE/PS-1 sample treated first according to the TP route. This sample, with two distinct populations of lamellae, was again pressurized and heated to a temperature outside the pseudohexagonal region 225 °C, via the PT route, annealed for 1 h and then cooled down to room temperature still under pressure, as is sketched in Figure 13. The DSC heating thermogram of this sample is also shown in Figure 13. The heating thermogram exhibited still two melting peaks, at lower and at higher temperature. This shows that the HDPE droplets inside the PS matrix were annealed indeed outside the region of pseudohexagonal phase stability, otherwise the low temperature peak would have vanished like in the other HDPE/PS-1 samples treated according to the PT route. The high temperature peak did not vanish either. If the pressure was not transferred to the thick crystals, they would have melted during heating to 225 °C and they would have recrystallized as orthorhombic crystals with melting temperature below 135 °C. This experiment demonstrated that application of the PT route enabled us to transform orthorhombic crystals to pseudohexagonal domains without melting.

We are also aware that the crystal thickness listed in Table 2 was calculated based on the Gibbs−Thomson formula with the assumption of constant lamellar basal free energy, 90 mJ/m^2, despite the fact that the basal surface of chain extended crystals was relatively free from chain folds. Hoffman et al.[28] developed a formula describing the free energy in terms of the number of chain folds and cilia. When only folds and chain ends form the PE lamellar basal plane, the value of σ_e is described by the following empirical formula:

$$\sigma_e = 93(f + 0.153)/(f + 1) \qquad [\mathrm{mJ/m^2}] \qquad (2)$$

where f is the number of folds per single macromolecule. It follows from eq 2 that if no folds are incorporated in the lamellar basal plane ($f = 0$), the value of σ_e is equal only to 14.2 mJ/m^2 instead of 90 mJ/m^2. Chain extended crystals have certainly decreased σ_e value, which would result in a smaller lamella thickness if calculated based on eq 1. Moreover, Bartczak and Kozanecki[29] suggested that the Gibbs−Thomson equation gives the stem length rather than the lamella thickness and that the correction for the tilt angle, approximately 35°,[30] should be introduced. Further, a lamella thickness distribution contributes to width of the melting peak during heating. There is also uncertainity concerning the $T_m°$ of PE crystals. The lower the $T_m°$ value assumed the larger the crystal thickness calculated based on eq 1. However, the experimental value used by us is slightly higher than the value of $T_m°$ calculated based on the Flory−Vrij equation for HDPE[31] for M_w of 125 000, equal to 144.98 °C. Nevertheless, even if eq 1 gives us only an approximate crystal thickness, it is evidently sufficient to differentiate between orthorhombic crystals crystallized under atmospheric pressure and crystals formed and/or thickened under high pressure.

Conclusions

In this study we examined crystallization of HDPE droplets under high pressure, in the region of the phase diagram where the pseudohexagonal phase is stable. The dispersions of HDPE droplets in PS were produced by melting and breakup of thin HDPE layers confined between thicker PS layers. The droplet size depended on thickness of the individual HDPE layers.

The pseudohexagonal phase was formed in HDPE control samples at selected conditions either from the melt or by transformation of orthorhombic crystals without prior melting. High pressure crystallization of HDPE droplets from the melt depended, however, on droplet sizes. The pseudohexagonal phase was found to form only in the relatively large droplets, obtained by melting 120 and 40 nm thick layers, that contained heterogeneities that nucleated HDPE crystallization in bulk. The submicron size droplets obtained by breakup of 14 nm thick layers were numerous enough that the majority did not contain those heterogeneities and crystallization under atmospheric pressure occurred in them primarily at about 80 °C, possibly by homogeneous nucleation. In these droplets the pseudohexagonal phase practically did not form under high pressure. In contrast to this, orthorhombic lamellae, if pressurized prior to heating, transformed to the pseudohexagonal phase in all the droplets, regardless of their size, however, the crystallinity level and lamella thickness were lower than those in the HDPE control sample. Although the decreasing droplet size limited the crystal thickness, it was still large enough to enable thickening of crystals. Therefore, we conclude that the growth of pseudohexagonal domains in the droplets was possible in spite of spatial confinement.The results indicate undoubtedly that, under the conditions of our experiments, heterogeneous nucleation was necessary for the formation of the pseudohexagonal phase of HDPE. It may be a general characteristic for the formation of pseudohexagonal phase.

Acknowledgment. This research was supported by the NSF Center for Layered Polymeric Systems (Grant DMR- 04923914, Polymers Program) and the Ministry of Education and Science, Poland (Grant 3T08E 059 29, 2005−2008).

References and Notes

(1) Bassett, D. C. On the Role of the Hexagonal Phase in the Crystallization of Polyethylene. *Adv. Polym. Sci.* **2005**, *180*, 1–16.

(2) Auriemma, F.; De Rosa, C.; Corradini, P. Solid Mesophases in Semicrystalline Polymers:Structural Analysis by Diffraction Techniques. *Adv. Polym. Sci.* **2005**, *181*, 1–74.

(3) Kazmierczak, T.; Galeski, A. Transformation of Polyethylene Crystals by High-Pressure Annealing. *J. Appl. Polym. Sci.* **2002**, *86*, 1337–1350.

(4) Bassett, D. C.; Khalifa, B. A. Chain-extended crystallization of polyethylene: effect of sample thickness. *Polymer* **1973**, *14*, 390–393.

(5) Khalifa, B. A.; Bassett, D. C. Morphological study of chain-extended growth in polyethylene: 3. Annealing of solution-grown lamellae. *Polymer* **1976**, *17*, 291–297.

(6) Jin, Y.; Hiltner, A.; Baer, E.; Masirek, R.; Piorkowska, E.; Galeski, A. Formation and Transformation of Smectic Polypropylene Nanodroplets. *J. Polym. Sci., Part B: Polym. Phys.* **2006**, *44*, 1795–1803.

(7) Silvestre, C.; Cimmino, S.; Duraccio, D. Schick, Ch. Isothermal Crystallization of Isotactic Poly(propylene) Studied by Superfast Calorimetry. *Macromol. Rapid Commun.* **2007**, *28*, 875–881.

(8) Koutsky, J. A.; Walton, A. G.; Baer, E. Nucleation of Polymer Droplets. *J. Appl. Phys.* **1967**, *38*, 1832–1839.

(9) Morales, R. A.; Arnal, M. L.; Muller, A. J. The evaluation of the state of dispersion in immiscible blends where the minor phase exhibits fractionated crystallization. *Polym. Bull.* **1995**, *35*, 379–386.

(10) Ghijsels, A.; Groesbeek, N.; Yip, C. W. Multiple crystallization behaviour of polypropylene/thermoplastic rubber blends and its use in assessing blend morphology. *Polymer* **1982**, *23*, 1913–1916.

(11) Santana, O. O.; Muller, A. J. Homogeneous nucleation of the dispersed crystallisable component of immiscible polymer blends. *Polym. Bull.* **1994**, *32*, 471–474.

(12) Arnal, M. L.; Matos, M. E.; Morales, R. A.; Santana, O. O.; Muller, A. J. Evaluation of the fractionated crystallization of dispersed polyolefins in a polystyrene matrix. *Macromol. Chem. Phys.* **1998**, *199*, 2275–2288.

(13) Arnal, M. L.; Muller, A. J. Fractionated crystallisation of polyethylene and ethylene/α-olefin copolymers dispersed in immiscible polystyrene matrices. *Macromol. Chem. Phys.* **1999**, *200*, 2559–2576.

(14) Arnal, M. L.; Muller, A. J.; Maiti, P.; Hikosaka, M. Nucleation and crystallization of isotactic poly(propylene) droplets in an immiscible polystyrene matrix. *Macromol. Chem. Phys.* **2000**, *201*, 2493–2504.

(15) Bernal-Lara, T. E.; Liu, R. Y. F.; Hiltner, A.; Baer, E. Structure and thermal stability of polyethylene nanolayers. *Polymer* **2005**, *46*, 3043–3055.

(16) Mueller, C.; Kerns, J.; Ebeling, T.; Nazarenko, S.; Hiltner, A.; Baer, E. Microlayer coextrusion: processing and applications. In *Polymer processing engineering 97*; Coates, P. D., Ed.; The Institute of Materials: London, 1997; pp 137−157.

(17) Ma, Y.; Hu, W.; Reiter, G. Lamellar Crystal Orientations Biased by Crystallization Kinetics in Polymer Thin Films. *Macromolecules* **2006**, *39*, 5159–5164.

(18) Hoffman, J. D. Regime III crystallization in melt-crystallized polymers: The variable cluster model of chain folding. *Polymer* **1983**, *24*, 3–26.

(19) Hoffman, J. D. Role of reptation in the rate of crystallization of polyethylene fractions from the melt. *Polymer* **1982**, *23*, 656–670.

(20) Psarski, M.; Piorkowska, E.; Galeski, A. Crystallization of Polyethylene from Melt with Lowered Chain Entanglements. *Macromolecules* **2000**, *33*, 916–932.

(21) Wunderlich, B.; Czornyj, G. A Study of Equilibrium Melting of Polyethylene. *Macromolecules* **1977**, *10*, 906–913.

(22) Kazmierczak, T.; Galeski, A.; Argon, A. S. Plastic deformation of polyethylene crystals as a function of crystal thickness and compression rate. *Polymer* **2005**, *46*, 8926–8936.

(23) Olley, R. H.; Bassett, D. C. An improved permanganic etchant for polyolefines. *Polymer* **1982**, *23*, 1707–1710.

(24) de Langen, M.; Prins, K. O. Mobility of polyethylene chains in the orthorhombic and hexagonal phases investigated by NMR. *Chem. Phys. Lett.* **1999**, *299*, 195–200.

(25) de Langen, M.; Prins, K. O. NMR investigation of phase transitions in polyethylene in the vicinity of the hexagonal high pressure phase. *Polymer* **2000**, *41*, 1175–1182.

(26) de Langen, M.; Luigjes, H.; Prins, K. O. High pressure NMR study of chain dynamics in the orthorhombic phase of polyethylene. *Polymer* **2000**, *41*, 1183–1191.

(27) Oels, H. J.; Rehage, G. Pressure-Volume-Temperature Measurements on Atactic Polystyrene. A Thermodynamic View. *Macromolecules* **1977**, *10*, 1036–1043.

(28) Hoffman, J. D.; Ross, G. S.; Frolen, L.; Lauritzen, J. I. On the growth rate of spherulites and axialites from the melt in polyethylene fractions: regime I and regime II crystallization. *J. Res. Natl. Bur. Stand.* **1975**, *79A*, 671–699.

(29) Bartczak, Z.; Kozanecki, M. Influence of molecular parameters on high-strain deformation of polyethylene in the plane-strain compression. Part I. Stress-strain behavior. *Polymer* **2005**, *46*, 8210–8221.

(30) Olley, R. H.; Hodge, A. M.; Basset, D. C. A permanganic etchant for polyolefines. *J. Polym. Sci., Polym. Phys. Ed.* **1979**, *17*, 627–643.

(31) Hoffman, J. D.; Miller, R. L. Kinetics of crystallization from the melt and chain folding in polyethylene fractions revisited: theory and experiment. *Polymer* **1997**, *38*, 3151–3212.

MA800933G